analytical chemistry

Technical Note

pubs.acs.org/ac

Fabrication of Carbon, Gold, Platinum, Silver, and Mercury Ultramicroelectrodes with Controlled Geometry

Laurence Danis,[†] David Polcari,[†] Annie Kwan, Samantha Michelle Gateman, and Janine Mauzeroll*

Department of Chemistry, McGill University, 801 Sherbrooke Street West, Montreal, Quebec, Canada H3A 0B8

Supporting Information

ABSTRACT: A simple, fast, and reproducible method for the fabrication of disk ultramicroelectrodes (UMEs) with controlled geometry is reported. The use of prepulled soda-lime glass capillaries allows one to bypass the irreproducible torch-sealing and experimentally challenging tip-sharpening steps used in conventional fabrication protocols. A micron-sized electroactive wire is sealed inside this capillary producing UMEs with a highly reproducible geometry. Total fabrication time (1 h) and experimental difficulty are significantly reduced. Disk UMEs with various diameters and cores were fabricated, including carbon fiber (7 and 11 μm), gold (10 and 25 μm), platinum (10 and 25 μm), silver (25 μm), and mercury (25 μm). The ratio of the insulating sheath to the electroactive core of the UMEs was 2.5−3.6. Silver UMEs were also used to produce a Ag/AgCl microreference electrode. This general fabrication method can readily be applied to other electroactive cores and could allow any research group to produce high quality disk UMEs, which are a prerequisite for quantitative scanning electrochemical microscopy.

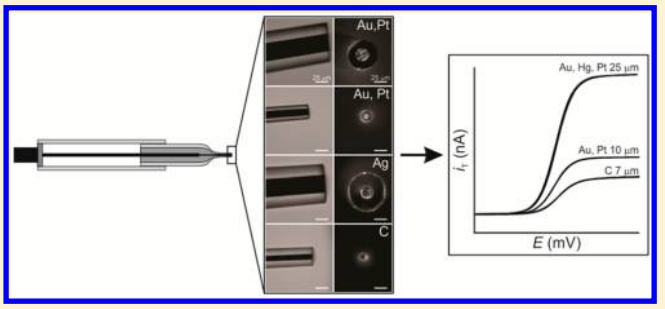

Ultramicroelectrodes (UMEs) are defined as electrodes with at least one dimension smaller than 25 μm.[1] They offer several advantages, including small size, high sensitivity, fast steady state response, low double-layer charging currents, and small ohmic losses.[2] The development and fabrication of UMEs has been the subject of several reviews.[3,4] Common geometries include disk,[5,6] hemispherical,[7,8] inlaid ring,[9,10] ring-disk,[11,12] and finite conical.[13,14] The most frequently used geometry is disk, whereby an electroactive material is embedded in a thin insulating layer. UMEs have been used in a variety of applications including biological systems,[15,16] charge transport at liquid/liquid interfaces,[17,18] and corrosion studies.[19,20]

The fabrication of high quality UMEs with an ideal geometry is a difficult and time-consuming process requiring experimental skill and patience. Alternatively, research groups can opt to purchase UMEs from commercial sources, but the price per UME is high (142−417 USD$). A critical geometric parameter affecting the overall quality of the UME is the *RG*, defined as the ratio between the radius of the insulating sheath (r_T) and the radius of electroactive surface (a). UMEs with small *RG* are essential in scanning electrochemical microscopy (SECM) to achieve minimal tip-to-substrate distances (d), allowing for a higher sensitivity.[21] The *RG* also has a significant effect on the current recorded during SECM approach curve measurements. A smaller *RG* will result in a larger current at short tip-to-substrate distances (<5) because of enhanced contributions from back diffusion of the mediator.[22] They also decrease the probability of contact between the insulating sheath of the UME and the sample, which experimentally occurs upon axial misalignment of the UME.[4]

There are two conventional techniques for the fabrication of gold or platinum disk UMEs. The first initially seals one end of a glass capillary (usually borosilicate or quartz) using a Bunsen burner or a torch. A metal wire is then inserted into the capillary and the glass is sealed around the metal wire using a heated coil. The UME tip is then polished to expose the electroactive surface using a polisher/grit paper. To minimize the *RG*, the electrode is sharpened by rotating over grit paper at a 45° angle.[3] This technique results in UMEs with an electroactive surface diameter ≥1 μm. The second UME fabrication technique involves sealing and pulling a metal wire inside a glass capillary using a laser-based micropipette puller system.[23]

We present herein a simple universal method for the fabrication of disk UMEs with various electroactive materials (platinum, gold, silver, mercury, and carbon fiber). This method produces highly reproducible UME geometries and decreases total fabrication time to less than 1 h. Importantly for SECM applications, the resulting disk UMEs have a small *RG* (2.5−3.6) with 90% yield. Moreover, the fabricated disk UMEs can be used as a geometrically controlled platform to develop other UME geometries. For example, the UMEs have been used as a backbone for the production of Hg disk UMEs and Ag/AgCl microreference electrodes.

Received: September 20, 2014
Accepted: January 28, 2015
Published: January 28, 2015

DOI: 10.1021/ac503767n
Anal. Chem. 2015, 87, 2565−2569

EXPERIMENTAL SECTION

Materials and Reagents. Gold and platinum wire (0.01 mm and 0.025 mm diameter; purity, 99.99%; temper, hard), silver wire (0.025 mm diameter; purity, 99.99%), and carbon fiber (0.011 mm diameter; Tex, 720; filaments, 4000; grade, P25; condition: epoxy sized) were purchased from Goodfellow. Carbon fiber (0.007 mm) was graciously donated by Bombardier. Soda-lime glass capillaries (AR8350; *L*, 75 ± 0.5 mm; o.d.,1.0 ± 0.05 mm; i.d., 0.4267 ± 0.05 mm; *S*, 0.2867 mm) and borosilicate capillaries (*L*, 75 mm; o.d., 2.0 mm; i.d., 1.16 mm) were purchased from Hilgenberg GmbH and Sutter Instruments, respectively. Abrasive polishing discs (4000 grit) and alumina powder (0.05, 0.1, 0.3, and 1.0 μm particle diameter) were purchased from Struers (Mississauga, Canada). Other materials included electrically conductive silver epoxy (EPO-TEK H20E; Epoxy Technology), copper wire (0.50 mm diameter), and gold connector pins (HEKA Elektronik). Ferrocenemethanol, potassium chloride, potassium nitrate, and hexaammineruthenium(III) chloride were purchased from Sigma-Aldrich. Other chemical reagents included nitric acid (10% v/v, Caledon Laboratories Ltd.) and mercury(I) nitrate dihydrate (Fisher Scientific).

Apparatus. UMEs were fabricated using a P-2000 laser-based micropipette puller system (Sutter Instruments), a PC-10-CA vertical pipette puller (Narishige, Japan) and a vacuum pump (Edwards RV8, Edwards). The electroactive surface was exposed and polished using a Tegrapol 23 variable speed grinder/polisher (Struers). All electrochemical measurements were performed using an Electrochemical Probe Scanner 3 (HEKA Elektronik) in a three-electrode setup with a platinum wire counter electrode. All potentials were recorded relative to a chloridized silver wire (in house) quasi-reference electrode, unless specified otherwise. Optical micrographs were obtained using a customized Axio Vert.A1 inverted microscope (Zeiss). The coil temperature was measured using a HH11B digital thermometer (OMEGA).

Preparation of Disk UMEs. A complete schematic of the disk UME fabrication technique is presented in Figure 1. Soda-lime glass capillaries were cleaned using 10% v/v nitric acid (1–2 h), rinsed with nanopure water, and dried in an oven (100 °C) for 12 h (Figure 1A). Using a P-2000 micropipette puller, a capillary was pulled using a single line heating and pulling program (Heat: 240; Fil: 5; Vel: 60; Del: 140; Pul: 70) (Figure 1B). Equal tensile force was applied at each end of the capillary along with simultaneous heat from a CO_2 laser, resulting in the production of two symmetric micropipette tips (Figure 1C). A 1 cm long section of electroactive material (Ag, Au, C, or Pt) was inserted into the pulled micropipette tip. By placing the assembly tip down and lightly tapping on the open extremity of the micropipette tip, the wire/fiber traveled downward until trapped in the sealed extremity. The assembly was then inserted into a PC-10-CA vertical pipette puller (Figure 1D). A vacuum pump was attached to the open end of the micropipette, and the pressure was reduced for 5 min to minimize bubble formation. The wire was sealed by centering the assembly inside a Kanthal (iron–chromium-aluminum) heating coil and applying heat for ∼10–20 s after maximum temperature was reached (bright orange coil) (Figure 1E). The sealed wire was connected to a Cu wire using conductive silver epoxy, which was subsequently cured at 120 °C for 15 min. The assembly was inserted into a larger borosilicate capillary to provide additional reinforcement, and the overlapping edges were sealed using 5 min epoxy. A gold connector pin was then soldered to the copper wire, completing the assembly (Figure 1F). The electroactive surface of the UME was exposed using a grinder/polisher (400 rpm, 4000 grit) followed by an alumina powder polishing.

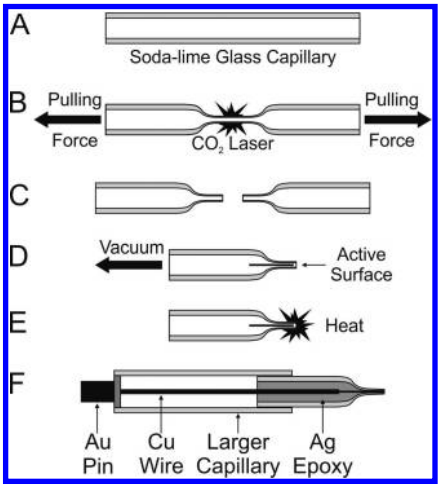

Figure 1. Schematic representation of pulling protocol: (A) Soda-lime glass capillaries. (B) Heat and a pulling force was applied to both ends of the capillary using a P-2000 Laser-Based Micropipette Puller. (C) Tapered micropipette tips following pulling. (D) Insertion and positioning of the wire inside the micropipette tip. (E) Sealing of the UME using a heating coil. (F) External and electrical connections; final UME assembly.

Preparation of Mercury Disk UMEs. Au disk UMEs (25 μm) were chemically etched by immersion in aqua regia (nitro-hydrochloric acid) solution for 10–20 min. The UME was rinsed with acetone and nanopure water to halt etching. Hg was then electrodeposited onto the recessed electroactive surface of the UME using the same procedure as for hemispherical UMEs (see the Supporting Information). However, the potential was applied for a longer period of time, such that a Hg hemisphere protruded from the glass. A disk was then formed by mechanically polishing the excess Hg. Disk UMEs were stored in a degassed, 0.5% acidified 0.1 M KNO_3 solution.

Preparation of Silver–Silver Chloride Microreference Electrodes. Bare 25 μm Ag disk UMEs were coated with silver chloride by immersion in a 1.0 M KCl solution with the application of 2.0 V in a two-electrode setup using a Pt wire counter electrode for 20 s according to the following reaction:

$$AgCl_{(s)} + e^- \leftrightarrow Ag_{(s)} + Cl^-_{(s)} \quad (1)$$

The microreference electrodes were stored in 0.1 M KCl when not in use.

Electrochemical Measurements. Electrochemical behavior was characterized by cyclic voltammetry and SECM approach curves. Ferrocenemethanol (FcMeOH; 1 mM) was used for Au, C, and Pt measurements, while hexaammineruthenium(III) chloride (ruhex; 1 mM) was used for measurements with Ag and Hg.

For cyclic voltammetry using FcMeOH, the potential was varied linearly from −100 to 400 mV, while a window of 0 to −500 mV versus Ag was used with ruhex. All cyclic voltammograms (CVs) were performed using a scan rate of 10 mV s^{-1}.

SECM approach curves were performed at constant potential of 400 mV for FcMeOH and −400 mV for ruhex (−450 mV vs

DOI: 10.1021/ac503767n
Anal. Chem. 2015, 87, 2565–2569

Ag for Hg). Negative feedback approaches were performed over solvent-resistant chlorotrifluoroethylene (CTFE) plastic, while positive feedback approach curves were performed over a 1.6 mm gold disk macroelectrode (MF-2014; BASi). The speed of approach used was 1 μm s^{-1}.

The electrochemical behavior of Hg hemispherical UMEs was characterized using cyclic voltammetry in ruhex from −300 to −900 mV versus Hg/Hg_2SO_4 (Figure S5 of the Supporting Information) at a scan rate of 10 mV s^{-1}. The full surface coverage of the Hg on the active material was characterized using linear sweep voltammetry (from 0 to −2.0 V vs Hg/Hg_2SO_4) in a 0.1 M KNO_3 solution (Figure S4 of the Supporting Information), whereby the proton reduction overpotential shifted to more negative potentials compared to a bare disk UME. In this case, potentials were recorded relative to a chloride free Hg/Hg_2SO_4 (sat. K_2SO_4) (REF 601, Radiometer Analytical) reference electrode. Information on the characterization of the hemispherical UMEs is located in the Supporting Information.

RESULTS AND DISCUSSION

Disk UME Characterization. The fabrication procedure (Figure 1) was tested by 10 subjects without any prior electrode fabrication experience whatsoever, yielding consistently high quality UMEs. Total fabrication time for a single UME was less than 1 h. However, several steps can be performed concurrently for several UMEs (e.g., epoxy curing), allowing for the production of a batch of 30 UMEs during a single day. UMEs were characterized using optical microscopy, cyclic voltammetry, and SECM approach curves. These three complementary techniques evaluate several important parameters, including the *RG*, quality of the polishing and sealing, and most importantly, the electrochemical behavior of the UME.

Side view images (Figure 2, panels A–D, left) confirm the absence of air bubbles and a proper concentric seal of the wire/fiber within the insulating glass sheath. The sealed length was 3–5 mm. To avoid capillary bending during sealing, concentric alignment of the UME within the heating coil and coil temperature (heater level 60.0 or 717 °C) were rigorously controlled. Bending effects were more prevalent when using smaller diameter wires. Top view optical micrographs (Figure 2, panels A–D, right) confirm ideal disk geometry with a well-centered electroactive core surrounded by an insulating sheath, requiring no further sharpening step as previously described.

To characterize the electrochemical behavior of the UMEs, cyclic voltammetry was used (Figure 2E). The steady state current (i_{ss}) is governed by the flux of redox species in solution toward the electrode surface as described by[22]

$$i_{ss} = knFaDC^*\beta \quad (2)$$

Where k is a geometric constant (disk, $k = 4$; hemispherical, $k = 2\pi$), n is the number of electrons involved in the reaction, F is the Faraday constant (96 485 C eq^{-1}), a is the radius of the electroactive surface, D is the diffusion coefficient of the redox species ($D_{FcMeOH} = 7.8 \times 10^{-6}$ cm^2 s^{-1}; $D_{Ruhex} = 8.7 \times 10^{-6}$ cm^2 s^{-1}),[8] C^* is the concentration of dissolved redox species, and β is a tabulated factor dependent on the *RG* of the UME. Using this equation and the experimental i_{ss} of the CVs (see Table 1), the diameters of the electroactive surface of the UMEs were calculated, as reported above the corresponding CVs in Figure 2E (all CVs are shown in Figure S2 of the Supporting Information). The calculated diameters are consistent with those observed in optical micrographs (Figure 2, panels A–D)

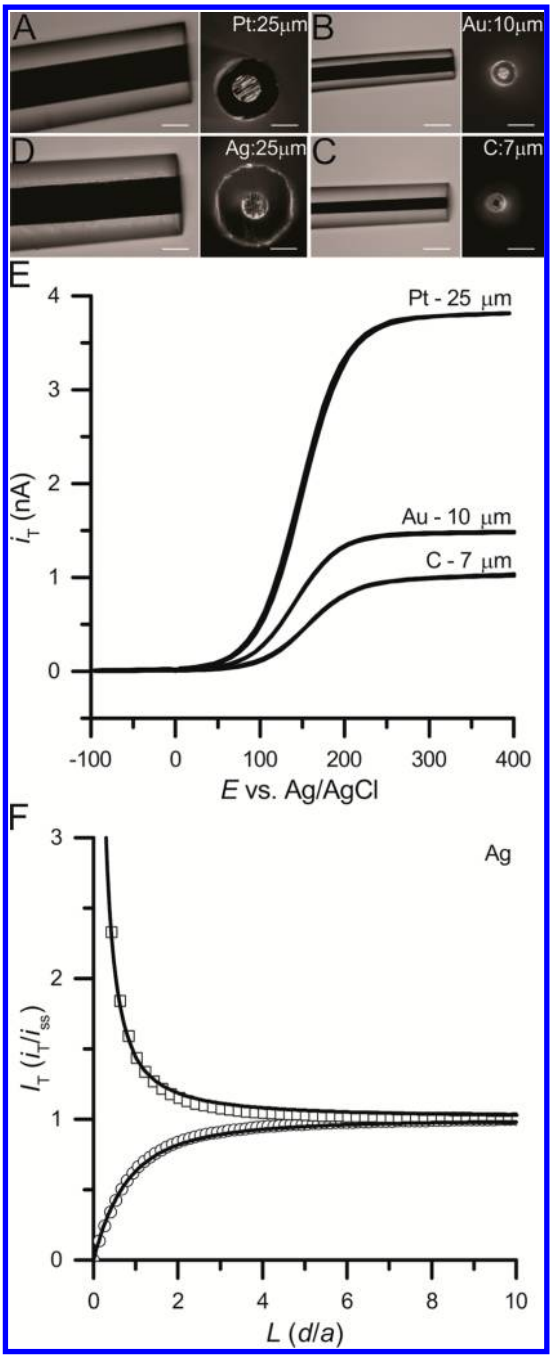

Figure 2. Characterization of disk UMEs. (A–D) Side and top view optical micrographs for various disk UMEs. Scale bars represent 25 μm. (E) Representative CVs for platinum (25 μm), gold (10 μm), and carbon (7 μm). CVs were performed using 1 mM FcMeOH in 0.1 M KCl at 10 mV sec^{-1}. (F) Negative (○) and positive (□) feedback approach curves for a silver disk UME performed using 1 mM $Ru(NH_6)^{3+}$ in 0.1 M KNO_3 with an AgQRE at a speed of 1 μm s^{-1}. Solid lines correspond to theoretical values obtained from an analytical expression.[22]

and reported by the manufacturer, confirming a high quality seal devoid of leaks and cracks, which would have manifested as an increased steady state current. This seal quality is further confirmed by the presence of a long current plateau over hundreds of millivolts. The lack of significant hysteresis in the CVs is also qualitatively indicative of a good polishing.

DOI: 10.1021/ac503767n
Anal. Chem. 2015, 87, 2565–2569

Table 1. *RG* of Experimental Disk UMEs

electroactive surface	electroactive surface diameter (μm)	*RG*	steady-state current (nA)	*n*
carbon	7	3.2 ± 0.1	1.07 ± 0.003	4
	11	2.5 ± 0.1	1.64 ± 0.02	3
gold	10	3.2 ± 0.2	1.51 ± 0.02	4
	25	2.7 ± 0.1	3.78 ± 0.04	5
platinum	10	3.6 ± 0.1	1.51 ± 0.02	5
	25	2.7 ± 0.1	3.70 ± 0.05	5
silver	25	2.7 ± 0.2	−4.47 ± 0.21	4
average	–	3.0 ± 0.2	–	30

SECM approach curves were used to determine *RG*. UMEs were approached toward an insulating or conducting surface while biased at a constant potential, producing negative and positive feedback currents, respectively (Figure 2F). The *RG* can be determined by fitting the experimental approach curves to theoretical expressions for current over an insulator or conductor.[22] The *RG* of fabricated disk UMEs were tabulated in Table 1. Using the proposed technique, UMEs with small *RG* are readily achievable. Moreover, the results in Table 1 indicate that the geometry of the fabricated UMEs is reproducible across electrode materials, with an average *RG* = 3.0 ± 0.2 (n = 30). The data is presented as mean ± standard error of the mean (S.E.M). The number of data points is defined as n. In comparison to a nonexhaustive compilation of commercially available SECM-grade disk UMEs (Table S1 of the Supporting Information), with only one exception, the *RG* of commercial disk UMEs are much larger than the ones reported in Table 1. Discussion on problems encountered when polishing Ag disk UMEs is reported in the Supporting Information.

Mercury Disk UME Characterization. Hg disk UMEs were fabricated using a combination of chemical etching, electrodeposition, and mechanical polishing. Optical micrographs were obtained at different stages of the fabrication process. The side view image (Figure 3A) highlights a chemically recessed Au UME. Etching depth can be adjusted by controlling the immersion time in aqua regia. Since the bare disk UMEs used during this fabrication process were previously characterized, it was determined that the diameter of the produced gap was equal to the diameter of the electroactive core (i.e., using a 25 μm Au disk UME, the diameter of the gap was also 25 μm). Following Hg electrodeposition and mechanical polishing, the side (Figure 3B) and top (Figure 3C) views of the optical micrographs confirm the disk geometry of the Hg UME. The top view (Figure 3C) also demonstrates that the Hg electroactive area is well-centered within the glass sheath. Following fabrication, Hg disk UMEs were characterized using CV (Figure 3D) and SECM approach curves (Figure 3E). Again, using equation 2 and the i_{ss} from the CV (Figure 3D), the diameter of the Hg disk UME was 25 μm, which is consistent with the diameter of the recessed Au wire backbone. The positive and negative feedback approach curves (Figure 3E) were fitted to theoretical expressions. The behavior of the Hg disk UME was equivalent to its Au disk UME backbone, with the same *RG*. The complete surface coverage of the Hg on the recessed gold surface was demonstrated using linear sweep voltammetry (Figure S4B of the Supporting Information), whereby a 650 mV overpotential cathodic shift in the proton reduction current is observed at the Hg UME as compared to the recessed disk UME.[24] The development of Hg

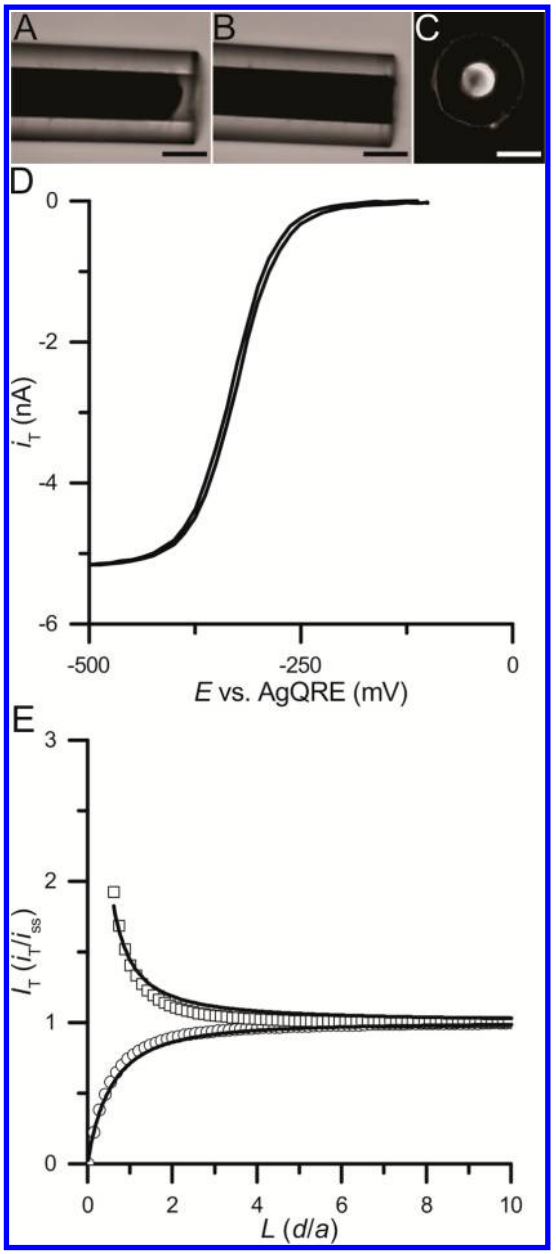

Figure 3. Characterization of Hg disk UMEs. (A) Side view optical micrograph of a recessed 25 μm Au disk UME following etching in aqua regia solution. (B) Side view optical micrograph of a Hg disk UME formed after electrodeposition and mechanical polishing. (C) Top view optical micrograph of a Hg disk UME. (D) CV of a Hg disk UME. (E) Negative (○) and positive (□) feedback approach curves for a Hg disk UME performed using ruhex at a speed of 1 μm s^{-1}. Solid lines correspond to theoretical values obtained from an analytical expression. Scale bars represent 25 μm.

disk UMEs allows for an extended solvent window in the negative potential region, which is not possible with conventional cores such as Au or Pt, and also offers an increase of sensitivity compared to other metals for the electroanalysis of trace metal.[25,26] Moreover the disk geometry allows fitting to established theoretical expressions. The method can also produce Hg hemispherical UMEs (see the Supporting Information).

Silver−Silver Chloride Microreference Electrode Characterization. Top and side view optical micrographs (Figure 4, panels A and B) show that an AgCl layer has successfully

DOI: 10.1021/ac503767n
Anal. Chem. 2015, 87, 2565−2569

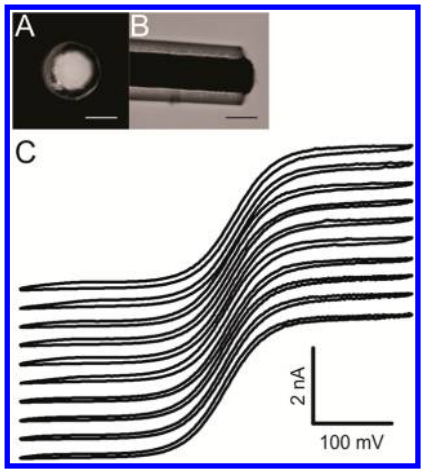

Figure 4. (A) Top and (B) side view optical micrograph of a 25 μm Ag/AgCl microreference electrode. (C) Steady-state voltammograms recorded using the same working electrode (25 μm Pt UME) and 10 different 25 μm Ag/AgCl microreference electrodes in FcMeOH. Scale bars represent 25 μm.

been electrodeposited onto the bare Ag disk UME. In order to evaluate the electrochemical stability of the microreference electrodes, cyclic voltammetry in FcMeOH was used. Figure 4C shows cyclic voltammograms obtained with 10 different microreference electrodes and the same working electrode (25 μm Pt disk UME). The exhibited electrochemical behavior is consistent with the response obtained from a commercial (and much larger) reference electrode. Even after 100 cycles, electrochemical response remained stable. The experimental $E^{0\prime}$ was calculated to be 166.9 $\pm$ 2.3 mV (n = 10). The small size of these microreference electrodes make them suitable for use in microelectrochemistry. Furthermore, using a double-barrel soft glass capillary with similar dimensions would allow fabrication of UMEs with an integrated Ag/AgCl microreference electrode.

CONCLUSIONS

We have successfully developed a general technique for the fabrication of disk UMEs with different electroactive cores, including carbon, gold, mercury, platinum, and silver. This technique leads to UMEs with small *RG* ranging from 2.5 to 3.6. The main advantages of the proposed fabrication technique include speed and relative ease of fabrication, controlled and reproducible geometry, and the ability to expand to multiple electroactive cores. Furthermore, the disk UMEs produced using this technique make them ideal backbones for surface-modified electrodes, demonstrated here by the production of Hg disk, hemispherical UMEs, and Ag/AgCl microreference electrodes. Finally, the optimal geometry of these probes makes them highly suitable for use in SECM measurements.

ASSOCIATED CONTENT

Supporting Information

Additional information as noted in text. This material is available free of charge via the Internet at http://pubs.acs.org.

AUTHOR INFORMATION

Corresponding Author

*E-mail: janine.mauzeroll@mcgill.ca. Tel: 514-398-3898. Fax: +1-514-398-3797.

Author Contributions

†L.D. and D.P. contributed equally to this work.

Notes

The authors declare no competing financial interest.

ACKNOWLEDGMENTS

This work was financially supported the Natural Sciences and Engineering Research Council of Canada (CRSNG) and by le Fonds québécois de la recherche sur la Nature et les technologies (FQRNT).

REFERENCES

(1) Bard, A. J.; Faulkner, L. R. *Electrochemical Methods: Fundamentals and Applications*. Wiley: New York, 1980; Vol. 2, p 169.
(2) Heinze, J. *Angew. Chem., Int. Ed.* **1993**, *32*, 1268−1288.
(3) Zoski, C. G. *Handbook of electrochemistry*; Elsevier: Amsterdam, 2007; Chapter 6.
(4) Zoski, C. G. *Electroanalysis* **2002**, *14*, 1041−1051.
(5) Danis, L.; Snowden, M. E.; Tefashe, U. M.; Heinemann, C. N.; Mauzeroll, J. *Electrochim. Acta* **2014**, *136*, 121−129.
(6) Katemann, B. B.; Schuhmann, W. *Electroanalysis* **2002**, *14*, 22−28.
(7) Velmurugan, J.; Noël, J. M.; Mirkin, M. V. *Chem. Sci.* **2014**, *5*, 189−194.
(8) Mauzeroll, J.; Hueske, E. A.; Bard, A. J. *Anal. Chem.* **2003**, *75*, 3880−3889.
(9) Takahashi, Y.; Shevchuk, A. I.; Novak, P.; Murakami, Y.; Shiku, H.; Korchev, Y. E.; Matsue, T. *J. Am. Chem. Soc.* **2010**, *132*, 10118−10126.
(10) Lee, Y.; Bard, A. J. *Anal. Chem.* **2002**, *74*, 3626−3633.
(11) Harvey, S. L. R.; Coxon, P.; Bates, D.; Parker, K. H.; O'Hare, D. *Sens. Actuators, B* **2008**, *129*, 659−665.
(12) Liljeroth, P.; Johans, C.; Slevin, C. J.; Quinn, B. M.; Kontturi, K. *Electrochem. Commun.* **2002**, *4*, 67−71.
(13) Fan, F. R. F.; Mirkin, M. V.; Bard, A. J. *J. Phys. Chem.* **1994**, *98*, 1475−1481.
(14) Mirkin, M. V.; Fan, F. R. F.; Bard, A. J. *J. Electroanal. Chem.* **1992**, *328*, 47−62.
(15) Zhao, X.; Diakowski, P. M.; Ding, Z. *Anal. Chem.* **2010**, *82*, 8371−8373.
(16) Kuss, S.; Polcari, D.; Geissler, M.; Brassard, D.; Mauzeroll, J. *Proc. Natl. Acad. Sci. U.S.A.* **2013**, *110*, 9249−9254.
(17) Sun, P.; Mirkin, M. V. *Anal. Chem.* **2006**, *78*, 6526−6534.
(18) Barker, A. L.; Unwin, P. R.; Zhang, J. *Electrochem. Commun.* **2001**, *3*, 372−378.
(19) Tefashe, U. M.; Snowden, M. E.; Ducharme, P. D.; Danaie, M.; Botton, G. A.; Mauzeroll, J. *J. Electroanal. Chem.* **2014**, *720−721*, 121−127.
(20) Eckhard, K.; Erichsen, T.; Stratmann, M.; Schuhmann, W. *Chem.—Eur. J.* **2008**, *14*, 3968−3976.
(21) Shen, M.; Arroyo-Currás, N.; Bard, A. J. *Anal. Chem.* **2011**, *83*, 9082−9085.
(22) Lefrou, C.; Cornut, R. *ChemPhysChem* **2010**, *11*, 547−556.
(23) Mezour, M. A.; Morin, M.; Mauzeroll, J. *Anal. Chem.* **2011**, *83*, 2378−2382.
(24) Velmurugan, J.; Mirkin, M. V. *ChemPhysChem* **2010**, *11*, 3011−3017.
(25) Rudolph, D.; Neuhuber, S.; Kranz, C.; Taillefert, M.; Mizaikoff, B. *Analyst* **2004**, *129*, 443−448.
(26) Wechter, C.; Osteryoung, J. *Anal. Chem.* **1989**, *61*, 2092−2097.

DOI: 10.1021/ac503767n
Anal. Chem. 2015, 87, 2565−2569